Oil Shale, 2010, Vol. 27, No. 3, pp. 194–208
doi: 10.3176/oil.2010.3.02 ISSN 0208-189X

GEOCHEMISTRY OF RARE EARTH ELEMENTS IN MARINE OIL SHALE – A CASE STUDY FROM THE BILONG CO AREA, NORTHERN TIBET, CHINA

XIUGEN FU[(a)*], JIAN WANG[(a)], YUHONG ZENG[(a,b)], FUWEN TAN[(a)], WENBIN CHEN[(a)], XINGLEI FENG[(a)]

[(a)] Chengdu Institute of Geology and Mineral Resources, Chengdu 610081, China
[(b)] College of Chemistry, Sichuan University, Chengdu 610065, China

The Bilong Co oil shale zone is located in the South Qiangtang depression. This zone, together with the Shengli River-Changshe Mountain oil shale zone in the North Qiangtang depression, northern Tibet plateau, represents a potentially large marine oil shale resource in China. The content and modes of occurrence of rare earth elements (REEs) in selected oil shale samples from the Bilong Co area were studied by inductively-coupled plasma mass spectrometer (ICP-MS) and statistical methods, respectively. The total organic carbon (TOC) content (6.75–19.20%) of oil shale samples is high with low or moderate total sulfur (St, d) content (1.05–2.00%) and intermediate shale oil content. The total rare earth element (∑REE) content of oil shale samples ranges from 63.69 to 117.85 μg/g. The average REE content of 13 oil shale samples from the Bilong Co area is slightly higher than that of USA coals and micritic limestone samples from the Bilong Co area, but lower than that of worldwide black shales. The oil shale samples from the Bilong Co area show shale-like chondrite or NASC-normalized REE patterns similar to those of micritic limestone samples from this area, indicating that REEs of these different lithological samples may have been derived from a similar terrigenous source. REE content of oil shale samples is highly positively correlated with ash yield and shows a positive correlation with Fe and a negative correlation with organic sulfur, and the vertical variations of REEs mainly follow those of Si, Al, K, Na and Ti. All these facts indicate that the REE content in oil shale seams is mainly controlled by clay minerals and, to a less extent, by pyrite, as well as partly associated with oil shale organic constituents.

Introduction

Oil shale as an alternative resource awaiting exploitation has received much attention [1–4]. In China, oil shale was formed mainly in lacustrine environ-

* Corresponding author: e-mail *fuxiugen@126.com*

ments, such as Tertiary oil shale in the Huadian [5] and Fushun areas [6], and Cretaceous oil shale in the Songliao basin [7]. Marine oil shale was mainly found in the Qiangtang basin, northern Tibet, China [8-10], including the Shengli River-Changshe Mountain oil shale zone and the Bilong Co oil shale zone. These zones represent a large marine oil shale resource in China. Therefore, studies of these oil shale zones are important for assessing petroleum prospects in the Qiangtang basin and the overall significance of marine oil shale researches in China.

In recent years, rare earth elements (REEs) in coal and shale have received much attention [11–12] owning to their stable geochemistry characteristics and potential economic value. Therefore, many researchers have studied REE geochemistry of different coals and shales [12–16]. However, little work has been done so far on the distribution of REEs in oil shale, especially in marine oil shale.

With the aim of better understanding geochemistry of marine oil shale, this paper investigates the content, modes of occurrence, and vertical variations of REEs in the Jurassic marine oil shale from the Bilong Co area.

Geological setting

The Qiangtang block, marked by Hoh Xil-Jinsha River suture zone to the north and Bangong Lake-Nujiang River suture zone to the south, respectively, consists of the North Qiangtang depression (North Qiangtang sub-basin), the central uplift and the South Qiangtang depression (South Qiangtang sub-basin) (Fig. 1a) [17]. The Bilong Co oil shale is located in the northern part of the South Qiangtang depression, northern Tibet plateau, China (Fig. 1a).

Jurassic strata are the most complete and extensive marine deposits in the Bilong Co area (Fig. 1b), including Lower Jurassic Quse Formation, Middle Jurassic Sewa Formation, Buqu Formation and Xiali Formation, and Upper Jurassic Suowa Formation. The Bilong Co oil shale was formed in the Early Jurassic time (i.e. Quse Formation strata) [18]. Sedimentary rocks of this stage are mainly made up of gypsum, shale, marl, micritic limestone, mudstone and oil shale.

Samples and analytical methods

The studied section is located in the Bilong Co area, the southern part of the Qiangtang basin (Fig. 1a). A total of 18 samples were collected from this section. Thirteen of them were collected from oil shale seams with a vertical sampling interval of 1 m on average, and the other five samples were collected from micritic limestone layers. All samples were collected and stored in plastic bags to ensure as little contamination and oxidation as possible.

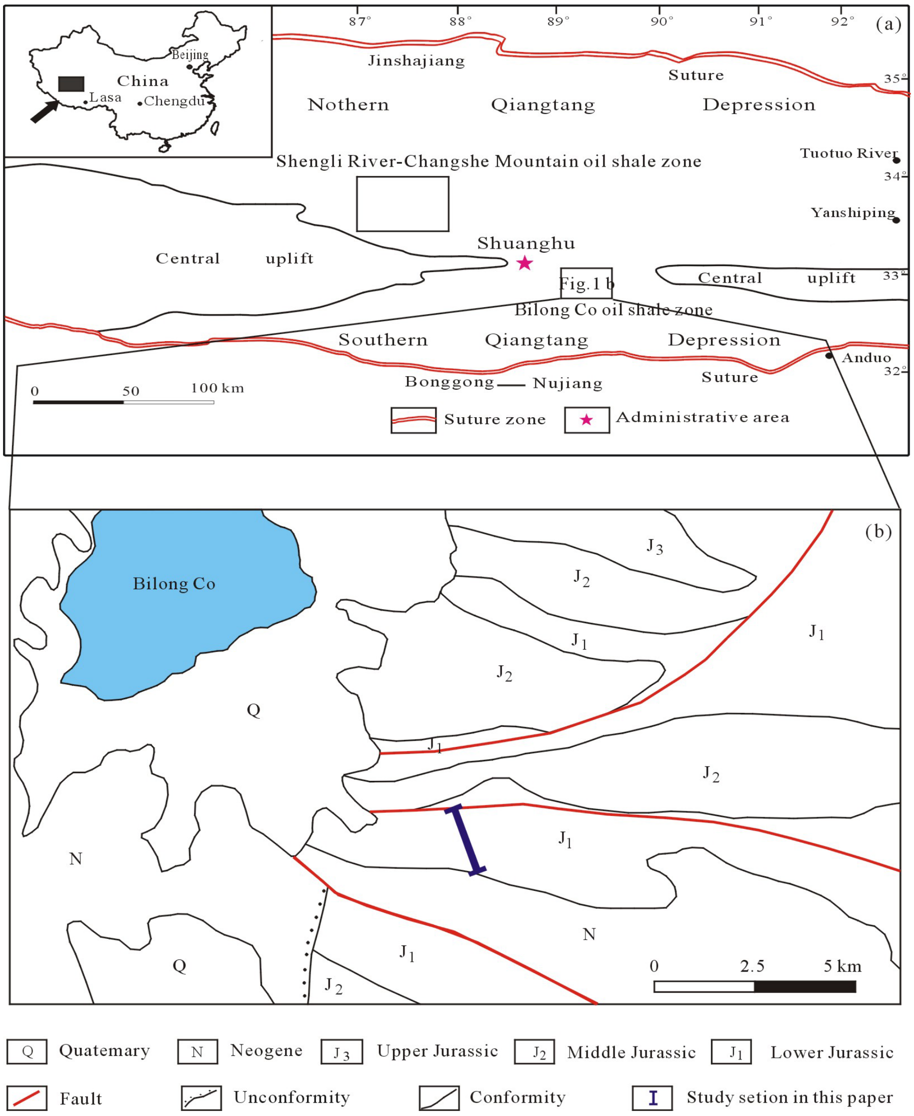

Fig. 1. (a) Generalized map showing location of study area. (b) Simplified geological map of the Bilong Co area showing location of oil shale section.

The samples for geochemical analysis were all crushed and ground to less than 200 mesh. Major element data were collected using X-ray fluorescence (XRF) on fused glass beads using a Rigaku ZSX100e spectrometer in the Analytical Center, Chengdu Institute of Geology and Mineral Resources. The analytical procedures are similar to those described by Kimura [19]. The analytical uncertainty is usually <5%. REE concentrations were determined by a Perkin Elmer Sciex Elan 6000 inductively-coupled plasma mass spectrometer (ICP-MS) at the Guangzhou Institute of Geochemistry, Chinese

Academy of Sciences, following the method of Qi *et al*. [14]. The analytical precision is generally within 5%. Ash yield and the content of total sulfur were conducted at the Coal Field Geological Bureau of Heilongjiang Province, following the Chinese standard methods GB/T212-2008 [20] and GB/T214-2007 [21], respectively. Organic sulfur and total organic carbon (TOC) were determined in the Geological Laboratory of Exploration and Development Research Institute of PetroChina Southwest Oil and Gas Field Company, using chemical method according to Chinese standards GB/T215-2003 [22] and GB/T19145-2003 [23], respectively. The mineral phases were determined by optical microscopic observation and powder X-ray diffraction spectrometer (XRD) (D8 ADVANCE using Cu Kα radiation set at 35 kV and 40 mA with a 3–50° 2θ range) at Tianjin Institute of Geology and Mineral Resources.

Results and discussion

Oil shale characterization and mineralogy

The TOC content of thirteen oil shale samples from the Bilong Co area varies from 6.75% to 19.20%, whereas micritic limestone samples contain 0.36-2.10% TOC (Table 1). The organic sulfur ($S_{o,\,d}$) content of oil shale and micritic limestone samples from the Bilong Co area varies from 0.37% to 0.48% and from 0.25% to 0.28%, respectively.

The analyses confirm that the Bilong Co oil shale samples exhibit high ash yields (58.88-71.96%) (Table 1) with low or moderate total sulfur ($S_{t,\,d}$) content (1.05-2.00%) (Table 1) and intermediate shale oil content (average 9.18%) [5].

There are a large variety of minerals in oil shale samples. Microscopic observation has revealed that the mineral component is normally higher than 45% by volume, ranging between 41.6% and 68.7%. These comprise mainly carbonates (19.8–42.3%), quartz (7.0–16.3%), clay minerals (21.2–36.5%) and pyrite (0.3–5.3%). Table 2 summarizes the semi-quantitative results of the mineral composition of the Bilong Co oil shale samples determined from the XRD analysis. Calcite, quartz, kaolinite and illite are the most abundant minerals (Table 2). Dolomite, pyrite, mix-layer clays, feldspars, anhydrite, as well as some weathering oxidation products such as haematite, are also present.

Major element geochemistry

Major element data in conjunction with mineralogical data may be used to establish the element-mineral associations for oil shale. Although the element associations may vary from one oil shale to another, a correlation analysis would demonstrate the general trends. The results of major element analysis of oil shale and micritic limestone samples are listed in Table 1. The major oxides in oil shale samples are dominated by SiO_2 (17.53–31.17%),

Table 1. **Concentrations of TOC, ash, total sulfur, organic sulfur and major elements in samples from the Bilong Co oil shale, %**

Sample nos.	Lithology	TOC	A_d	$S_{t,d}$	$S_{o,d}$	SiO_2	Al_2O_3	CaO	MgO	K_2O	Na_2O	TiO_2	P_2O_5	MnO	Fe	LOI
BP-6	Micritic limestone	1.67	67.09	1.88	0.28	23.23	7.69	28.93	0.76	1.45	0.32	0.29	0.12	0.035	2.81	33.1
BP-7-1	Oil shale	6.75	65.96	1.14	0.42	20.14	6.90	32.31	0.84	1.18	0.19	0.26	0.099	0.037	2.31	34.34
BP-7-2	Oil shale	7.23	65.32	1.13	0.43	19.20	6.46	33.25	0.84	1.12	0.20	0.25	0.10	0.038	2.24	34.98
BP-7-3	Oil shale	6.91	64.05	1.12	0.46	19.30	6.58	32.70	0.82	1.18	0.20	0.25	0.10	0.039	2.21	36.11
BP-8	Micritic limestone	1.36	66.08	1.77	0.28	19.66	6.12	33.38	0.78	1.17	0.26	0.23	0.12	0.036	2.6	34.03
BP-9	Micritic limestone	0.36	61.61	0.87	0.25	8.14	2.79	47.38	0.76	0.65	0.11	0.12	0.049	0.037	0.92	38.47
BP-10-1	Oil shale	19.20	62.99	2.00	0.47	21.67	7.88	22.64	0.74	1.36	0.30	0.31	0.34	0.033	4.17	38.72
BP-10-2	Oil shale	7.95	67.76	1.05	0.43	21.86	7.82	32.08	0.98	1.46	0.26	0.31	0.12	0.042	1.96	32.56
BP-10-3	Oil shale	7.66	69.59	1.37	0.42	25.39	8.63	27.46	0.76	1.55	0.37	0.35	0.22	0.034	2.68	31.34
BP-10-4	Oil shale	9.11	71.96	1.42	0.37	31.17	10.87	20.71	0.82	2.09	0.34	0.46	0.20	0.036	3.27	28.57
BP-11	Micritic limestone	2.10	60.12	0.88	0.26	5.56	1.66	48.40	1.05	0.44	0.083	0.080	0.14	0.053	1.09	40
BP-12-1	Oil shale e	10.27	62.06	1.41	0.46	20.06	7.20	27.00	0.84	1.27	0.33	0.29	0.24	0.040	3.22	38.06
BP-12-2	Oil shale	10.66	63.63	1.32	0.45	19.93	7.25	29.00	0.77	1.31	0.27	0.29	0.30	0.038	2.94	36.53
BP-12-3	Oil shale	7.13	71.44	1.46	0.43	28.58	10.26	23.50	0.89	1.91	0.37	0.42	0.21	0.042	3.47	28.77
BP-13	Micritic limestone	1.24	60.27	0.95	0.27	7.82	2.64	40.21	6.52	0.44	0.13	0.11	0.086	0.087	1.19	39.9
BP-14-1	Oil shale	10.96	64.58	1.19	0.43	20.44	7.08	30.76	0.90	1.24	0.21	0.29	0.12	0.038	2.49	35.64
BP-14-2	Oil shale	8.80	64.91	1.34	0.48	19.64	7.17	30.40	1.12	1.25	0.31	0.29	0.17	0.047	2.57	35.83
BP-14-3	Oil shale	13.50	58.88	1.52	0.45	17.53	6.55	26.60	0.72	1.08	0.30	0.28	0.35	0.034	3.04	42.13

TOC, Total organic carbon; A_d, ash yield, dry basis; $S_{t,d}$, total sulfur, dry basis; $S_{o,d}$, organic sulfur, dry basis; LOI, loss on ignition.

Table 2. **Mineral content (%) as inferred from semi-quantitative XRD analysis**

Seams	Kaolinite	Illite	Calcite	Dolomite	Quartz	Pyrite	Haematite	Feldspar	Anhydrite
BP-7-1	7.8	16.3	47.3	0.5	11.5	0.4	0.5		
BP-7-2	6.4	14.2	42.5	1.2	7.0	1.2		1.3	0.4
BP-7-3	6.2	15.7	46.2	1.5	16.1	5.3			
BP-10-1	5.4	18.5	44.7		6.8	0.7			0.7
BP-10-2	5.7	21.3	31.5	2.1	15.2	0.3			0.6
BP-10-3	6.1	19.6	48.5		13.5	0.5			
BP-12-1	3.1	12.4	47.5		11.2	3.2		0.6	0.6
BP-12-2	4.3	13.5	44.7		7.8	1.1		0.3	

Al_2O_3 (6.46–10.87%) and CaO (20.71–33.25%), and Fe and K are the second most abundant elements, while all other oxides (MgO, Na_2O, TiO_2, P_2O_5 and MnO) have a concentration of almost <1.0%. In contrast, major elements from micritic limestone samples exhibit a higher CaO concentration (28.93–48.40%), and slightly lower SiO_2 (5.56–23.23%), Al_2O_3 (1.66–7.69%) and Fe (0.92–2.81%) concentrations, while all other oxides (MgO, K_2O, Na_2O, TiO_2, P_2O_5 and MnO) have a concentration of almost <1.0%.

In the Bilong Co oil shale, most major elements show positive correlation with ash yield at 95% confidence level; they are SiO_2 (r = 0.88), Al_2O_3 (r = 0.83), K_2O (r = 0.85), Na_2O (r = 0.36) and TiO_2 (r = 0.77) (Table 3), indicating that these elements are mainly associated with minerals.

The elements Si, Al, Ti, K and Na are mainly associated with quartz and clay minerals. The significantly positive correlations among all these elements (Table 3) demonstrate that Si, Al, K, Na and Ti originate mainly from a mixed clay assemblage, which is consistent with the occurrence of kaolinite, illite, and illite/smectite mixed layers identified by the XRD analysis. The Al/Si ratios of oil shale and micritic limestone samples are low (0.38–0.42), suggesting that SiO_2 has another source in addition to clay minerals. The abundant quartz identified by the XRD analysis suggests that the extra SiO_2 is present in the form of quartz.

Two major elements showing a very close relationship are iron and total sulfur. The correlation coefficient (0.94) (Table 3) is highly significant. Iron and sulfur content increases together reflecting the abundance of pyrite, which is consistent with the occurrence of pyrite identified by the XRD analysis. Additionally, the results of this study also show that there is a significant correlation between iron and SiO_2 (r = 0.37), Al_2O_3 (r = 0.46), K_2O (r = 0.39), Na_2O (r = 0.62) and TiO (r = 0.48) (Table 3), indicating that iron is also present in the clay minerals.

Calcium displays a positive correlation with MgO (r = 0.35) and MnO (r = 0.35) and appears to be related to the Ca-bearing minerals such as calcite, present in all the samples. Calcium is believed to be present in more than one form such as carbonates and organic association, as inferred by Mukhopadhyay *et al*. [24]. Note that oil shale samples BP-7-1, BP-7-2, BP-7-3, BP-10-2, BP-14-1 and BP-14-2 contain much CaO (Table 1) corresponding to abundant bivalve and gastropod fossil remains, which suggests that Ca is also related to the fossil remains.

In the Bilong Co oil shale, positive relationships have been recorded between organic sulfur and Ca (r = 0.27), P (r = 0.27), Mn (r = 0.30) and Fe (r = 0.23) indicating that these elements are also present in organic matter. However, the correlation coefficients between organic sulfur and Ca, P, Mn and Fe are low, suggesting that these elements have another source in addition to organic association. The close relationships between total sulfur and P_2O_5 and Fe and the slightly positive correlations between CaO and MgO and MnO further support the above recognition.

Table 3. **The correlation coefficients of ash, total sulfur, organic sulfur, ∑REE and major element content of oil shale samples**

	A_d	$S_{t,d}$	$S_{o,d}$	∑REE	SiO_2	Al_2O_3	CaO	MgO	K_2O	Na_2O	TiO_2	P_2O_5	MnO	Fe
A_d	1.00													
$S_{t,d}$	–0.18	1.00												
$S_{o,d}$	–0.71	0.26	1.00											
∑REE	0.63	0.40	–0.49	1.00										
SiO_2	0.88	0.20	–0.70	0.87	1.00									
Al_2O_3	0.83	0.29	–0.63	0.92	0.99	1.00								
CaO	–0.29	–0.79	0.27	–0.82	–0.69	–0.76	1.00							
MgO	0.23	–0.41	0.18	0.03	–0.02	–0.01	0.35	1.00						
K_2O	0.85	0.21	–0.65	0.90	0.98	0.99	–0.71	0.03	1.00					
Na_2O	0.36	0.56	–0.10	0.81	0.62	0.69	–0.77	–0.06	0.65	1.00				
TiO_2	0.77	0.31	–0.63	0.96	0.96	0.99	–0.79	–0.02	0.98	0.73	1.00			
P_2O_5	–0.37	0.82	0.27	0.33	0.02	0.14	–0.67	–0.53	0.07	0.58	0.20	1.00		
MnO	0.16	–0.43	0.30	–0.03	–0.07	–0.03	0.35	0.91	0.02	–0.001	–0.05	–0.44	1.00	
Fe	–0.03	0.94	0.23	0.54	0.37	0.46	–0.89	–0.42	0.39	0.62	0.48	0.79	–0.36	1.00

REE parameters

The concentration of REEs and Y of 18 samples from the Bilong Co oil shale is presented in Table 4. The content of total rare earth elements (∑REE) of oil shale samples varies from 63.69 to 117.85 μg/g, with a mean value of 86.16 μg/g, slightly higher than 62.1 μg/g for the USA coals estimated by Finkelman [25], but lower than 134.19 μg/g for the world black shales calculated by Ketris and Yudovich [16]. In comparison of the ∑REE of the North American Shale Composite (NASC), the ∑REE of oil shale samples is notably depleted, approximately one third of the mean value (173.2 μg/g) of the NASC [26]. Compared with REE concentration in oil shale samples, the REE concentration in micritic limestone samples from the Bilong Co area is a little lower, ranging from 26.25 to 71.81 μg/g, with an average of 45.80 μg/g.

The concentration of the light rare earth elements (LREEs) is higher than that of the heavy ones, which is in accordance with the general distribution of REEs in shale [15–16, 27]. The LREE/HREE (heavy REE) ratios of oil shale samples from the Bilong Co area vary from 7.80 to 9.71, similar to those of micritic limestone samples. Both oil shale and micritic limestone samples exhibit a negative Eu anomaly (Table 4), with a mean δEu value of 0.65. The δCe values of all samples very from 0.97 to 1.01, showing a negligible Ce anomaly.

REE distribution patterns

All oil shale samples show similar chondrite-normalized REE patterns and have clearly fractionated LREEs relative to HREEs, showing a distinct negative Eu anomaly (Fig. 2a). These patterns are generally similar to those of micritic limestone samples from the Bilong Co area (Fig. 2b). Especially, when normalized to NASC, these oil shale and micritic limestone samples generally show shale-like or slightly LREE-rich patterns (Fig. 3a, b), and a lower Eu anomaly (the values of δEu range from 0.94 to 1.08) in comparison to the chondrite-normalized one, indicating that REEs of these different lithological samples may have been derived from a similar terrigenous source and the Eu anomaly was inherited from the source rocks [29]. When normalized to the average compositions of micritic limestone from the Bilong Co area, approximately three quarters of total oil shale samples show horizontal REE patterns, whereas a quarter (e.g., BP-7-1, BP-7-2 and B-7-3) of total samples displays a slight depletion in middle-REE (Fig. 4), indicating that small quantity of middle-REEs may be decreased and/or retain during epigenesis [30].

Table 4. **Rare earth element content (in µg/g) in samples and associated geochemical parameters**

Sample nos.	Lithology	La	Ce	Pr	Nd	Sm	Eu	Gd	Tb	Dy	Ho	Er	Tm	Yb	Lu	Y	ΣREE	L/H	$(La/Yb)_n$	Ce/Ce*	Eu/Eu*
BP-6	Micritic limestone	15.3	31	3.38	12.5	2.35	0.45	2.14	0.29	1.74	0.34	1.06	0.15	0.97	0.14	10.6	71.81	9.51	8.82	0.98	0.60
BP-7-1	Oil shale	14.5	29.2	3.16	11.9	2.07	0.42	1.96	0.28	1.73	0.34	0.99	0.14	0.9	0.13	10	67.72	9.47	8.94	0.98	0.63
BP-7-2	Oil shale	13.7	27.7	3.04	11.2	1.95	0.4	1.87	0.26	1.5	0.3	0.94	0.13	0.84	0.13	9.64	63.96	9.71	8.48	0.97	0.63
BP-7-3	Oil shale	13.8	27.5	2.99	11.2	2.05	0.41	1.87	0.26	1.58	0.31	0.92	0.14	0.88	0.13	9.19	64.04	9.52	8.42	0.97	0.63
BP-8	Micritic limeston	12.9	26.1	2.84	10.4	1.86	0.42	1.78	0.25	1.51	0.29	0.86	0.13	0.8	0.11	8.97	60.25	9.51	9.45	0.98	0.70
BP-9	Micritic limestone	7.37	14.7	1.57	5.83	1.19	0.23	1.19	0.16	0.97	0.18	0.54	0.07	0.5	0.07	5.32	34.57	8.39	8.36	0.97	0.58
BP-10-1	Oil shale	18.2	38.6	4.07	15.2	2.86	0.64	2.71	0.38	2.36	0.44	1.22	0.18	1.17	0.18	13	88.21	9.21	8.54	1.02	0.69
BP-10-2	Oil shale	18.8	38.2	4.04	15.2	2.68	0.55	2.47	0.38	2.16	0.44	1.25	0.18	1.18	0.17	12.7	87.70	9.66	8.95	0.99	0.64
BP-10-3	Oil shale	20	41.6	4.48	16.6	3.61	0.73	3.34	0.49	2.6	0.5	1.47	0.2	1.29	0.18	15.6	97.09	8.64	9.20	1.00	0.63
BP-10-4	Oil shale	25	50.5	5.47	20.4	3.87	0.79	3.71	0.54	2.98	0.61	1.79	0.25	1.7	0.24	18.1	117.85	8.97	8.38	0.98	0.63
BP-11	Micritic limestone	5.31	10.8	1.2	4.65	0.93	0.23	0.98	0.14	0.82	0.17	0.45	0.07	0.44	0.06	5.16	26.25	7.39	7.17	0.97	0.73
BP-12-1	Oil shale e	17.5	36.1	3.81	14.6	2.99	0.65	3.15	0.42	2.55	0.51	1.38	0.21	1.25	0.2	15	85.32	7.82	7.19	1.00	0.64
BP-12-2	Oil shale	16.8	34.9	3.73	13.5	2.61	0.57	2.74	0.38	2.16	0.45	1.23	0.19	1.15	0.17	12.9	80.58	8.51	8.17	1.00	0.65
BP-12-3	Oil shale	23.5	48.7	5.14	19.3	3.77	0.73	3.5	0.47	2.94	0.58	1.68	0.24	1.43	0.23	17.6	112.21	9.14	8.43	1.00	0.60
BP-13	Micritic limestone	7.23	14.8	1.66	6.41	1.33	0.31	1.42	0.19	1.16	0.22	0.68	0.09	0.56	0.08	7.23	36.14	7.21	7.37	0.97	0.69
BP-14-1	Oil shale	17.9	37.1	4.1	15.5	3.04	0.64	3.08	0.42	2.4	0.47	1.33	0.19	1.23	0.2	13.7	87.60	8.40	7.39	0.99	0.63
BP-14-2	Oil shale	17.3	35.5	3.89	15.2	2.96	0.63	2.97	0.4	2.34	0.46	1.24	0.17	1.17	0.17	13.9	84.40	8.46	8.31	0.98	0.64
BP-14-3	Oil shale	16.5	35.2	3.8	14.8	2.96	0.67	3.23	0.44	2.57	0.49	1.29	0.18	1.11	0.17	14.1	83.41	7.80	8.24	1.01	0.66

L/H=LREE/HREE; $(La/Yb)_n$, subscript n stands for chondrite-normalized value; $Ce/Ce^*=Ce_n/(La_n \times Pr_n)^{0.5}$; $Eu/Eu^*=Eu_n/(Sm_n \times Gd_n)^{0.5}$.

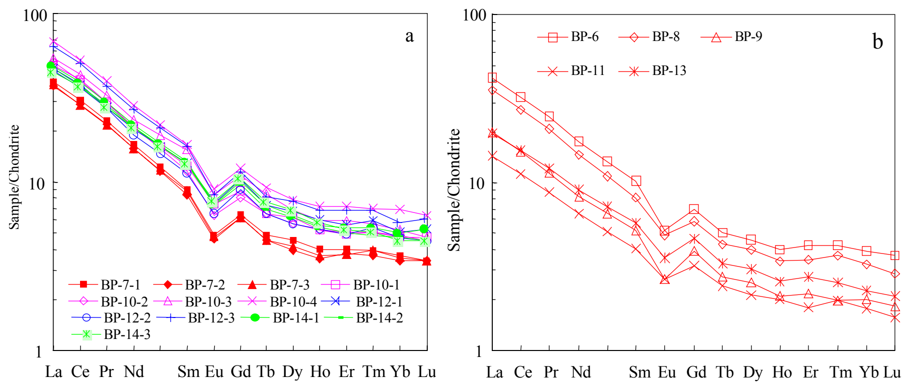

Fig. 2. Distribution patterns of rare earth elements in oil shale (a) and micritic limestone (b) samples from the Bilong Co area. Chondrite values after Taylor and Mcleman [28].

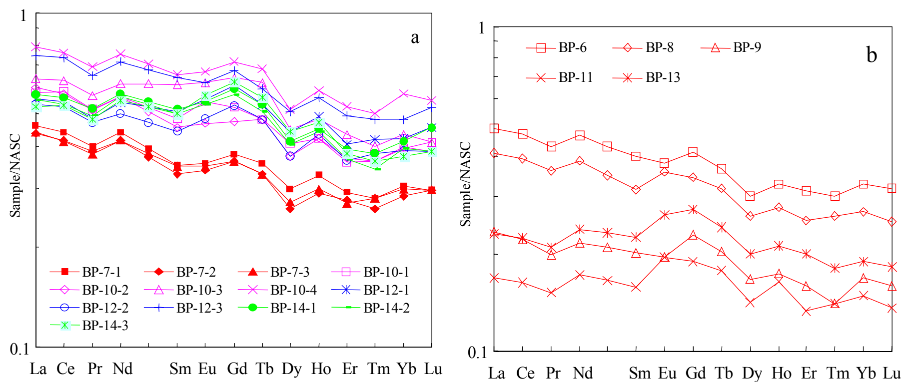

Fig. 3. NASC-normalized REE patterns of oil shale (a) and micritic limestone (b) samples from the Bilong Co area. NASC values after Haskin *et al*. [26].

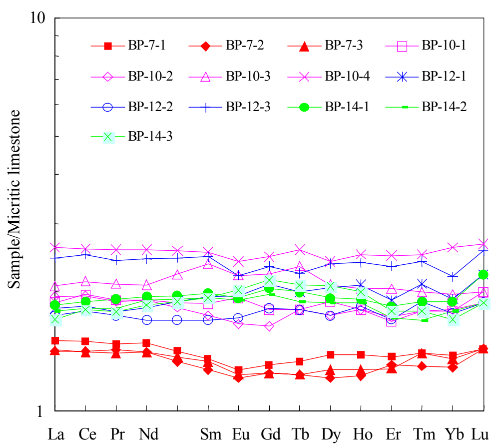

Fig. 4. Micritic limestone-normalized REE patterns of oil shale samples from the Bilong Co area.

Vertical distribution of the elements

The vertical distributions of the investigated elements in selected section are shown in Fig. 5.

(1) Although not a consistent pattern, ∑REE content generally increases from micritic limestone layer to oil shale seam (e.g., from ply BP-9 to ply BP-10-1; Table 4). Similar vertical variations are observed for ash, Si, Al, K, Na and Ti, which are attributed to a change of deposition conditions. Influenced by regional tectonics, sea level fluctuations in the Qiangtang basin were frequent during the Early Jurassic time [17], leading to different depositional environments from micritic limestone to oil shale. Therefore, seawater invasions may play an important role in controlling the content of Si, Al, K, Na, Ti and REEs.

(2) The vertical variations of total sulfur are similar to that of Fe, which is attributed to the presence of some pyrite crystals in the oil shale seams.

(3) Oil shale samples exhibit high organic sulfur content, whereas the content for the micritic limestone samples is lower. Similar vertical variations are observed for P. P is useful nutrients for plant growth [31], and P may be regarded as an element associated with high productivity [32–33]. The combination of high productivity and anoxic environment is in favour of the deposition of oil shale [10] and this could explain the consistent variations between organic sulfur content and P content.

(4) Micritic limestone samples exhibit high calcium content, whereas the content of oil shale samples is lower. The vertical variations of calcium show positive correlations with organic sulfur, ash, Mg and Mn content, suggesting that calcium is present in different phases.

The mode of occurrence of REE

Coarse-grained detrital minerals are rare in the Bilong Co oil shale; the absorption of fine-grained minerals and organic matter may be the main mode of occurrence of REEs. The individual REE contents of oil shale samples from the Bilong Co area are highly positively correlated with Al content (Fig. 6). The correlation coefficients range from 0.69 to 0.96, indicating that REEs of oil shale samples occur mainly in clay minerals. The significantly positive correlations between ∑REE and ash, SiO_2, K_2O, Na_2O and TiO_2 (Table 3) content further support the above recognition. A positive correlation between ∑REE and Fe content indicates that REEs occur partly in pyrite.

In contrast, the content of ∑REE in oil shale samples shows a negative correlation with organic sulfur, with the coefficient of -0.49 (Table 3). In reductive depositional environments, ferrous Fe reacts preferentially with H_2S resulting in the formation of iron sulfides, whereas H_2S reacts with organic matter to produce organic sulfur under high H_2S and low ferrous iron concentrations [11]. As discussed above, Fe in oil shale samples from the

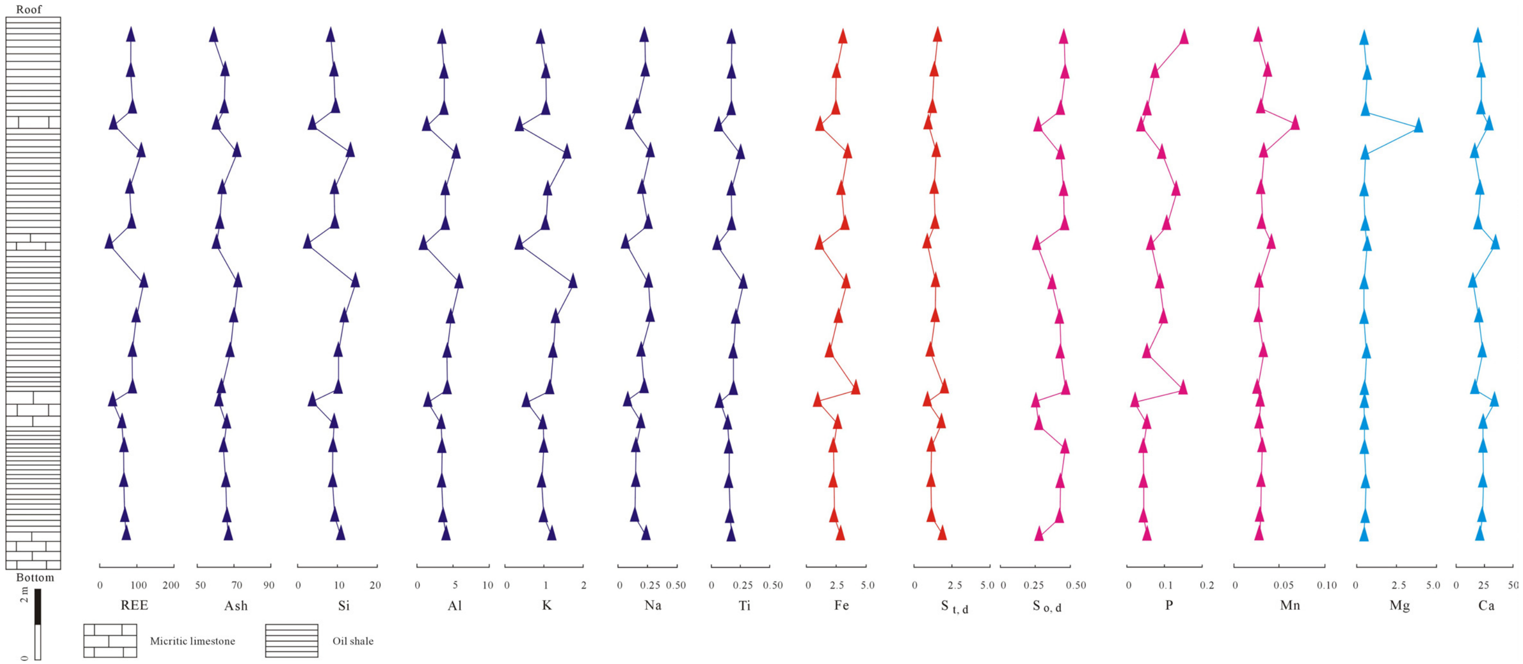

Fig. 5. Vertical variations of ash, total sulfur, organic sulfur, ∑REE and selected major elements in the Bilong Co oil shale section (REE in µg/g, the others in %).

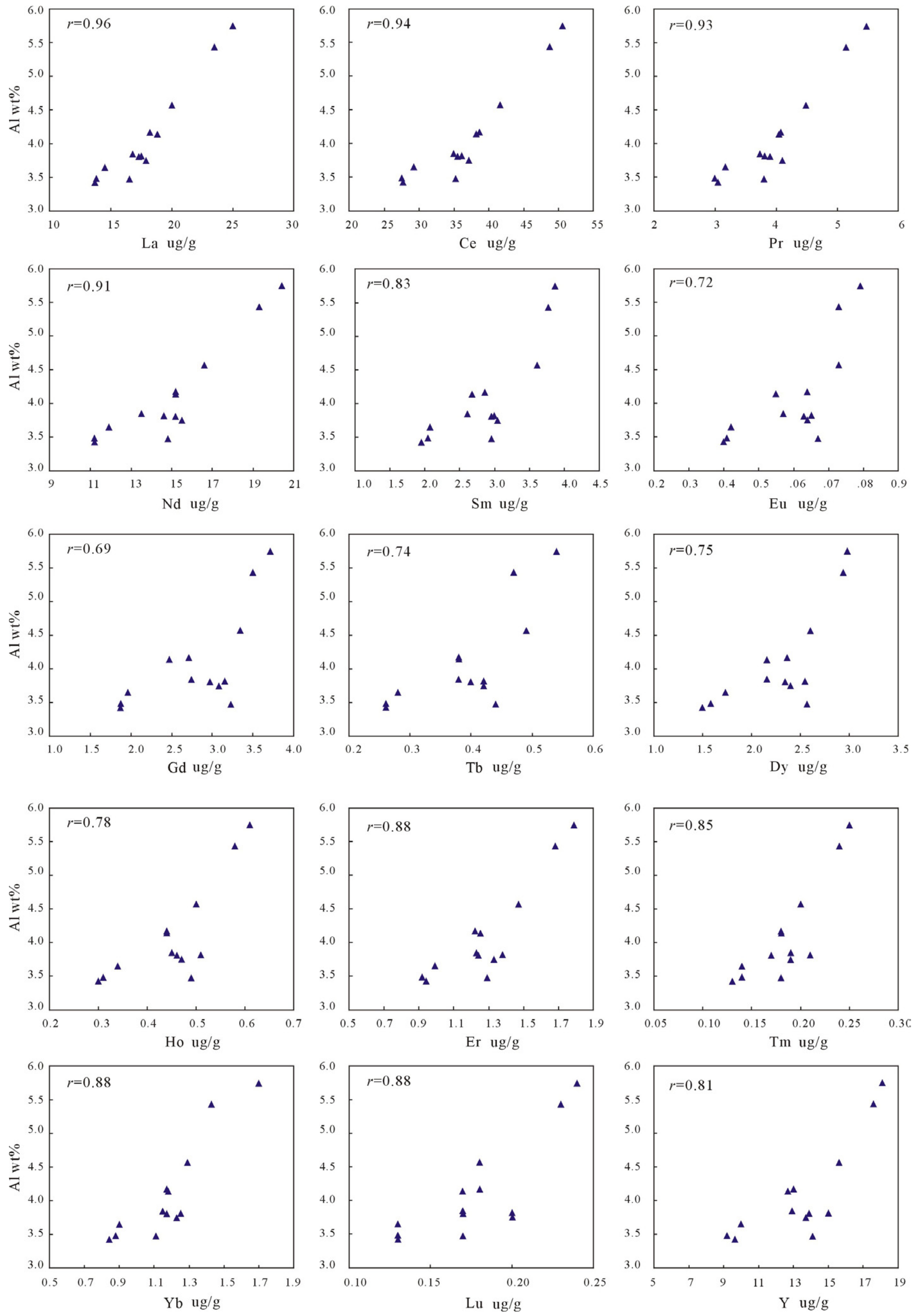

Fig. 6. Scatter diagrams of Al content against rare earth elements of oil shale samples from the Bilong Co area.

Bilong Co oil shale is present in the pyrite and the ferric ion-containing clay minerals. Consequently, low clay mineral abundance can lead to the formation of organic sulfur when enough H_2S is supplied [11], and this could explain the negative correlation between ΣREE and organic sulfur in oil shale samples.

Conclusions

1. The Bilong Co oil shale samples are characterized by high ash yield (58.88–71.96%) and TOC content (6.75–19.20%) with low or moderate total sulfur ($S_{t,\,d}$) content (1.05–2.00%) and intermediate shale oil content.
2. The content of ∑REE in oil shale samples varies from 63.69 to 117.85 μg/g, with an arithmetic mean value of 86.16 μg/g, and it is slightly higher than that of USA coals, but lower than that of worldwide black shales. In contrast, the REE concentration in micritic limestone samples from the Bilong Co area is a little lower, with an average of 45.80 μg/g.
3. The oil shale samples from the Bilong Co area have shale-like chondrite or NASC-normalized REE patterns similar to those of micritic limestone samples from this area, indicating that REEs of these different lithological samples may have been derived from a similar terrigenous source.
4. The vertical variations of REEs mainly follow those of ash, Si, Al, K, Na and Ti, and REE content of oil shale samples shows a positive correlation with Fe and a negative correlation with organic sulfur, suggesting that REEs of oil shale seams occur mainly in clay minerals and, to a less extent, in pyrite, as well as are partly influenced by oil shale organic constituents.

Acknowledgements

This work was supported by the National Natural Science Foundation of China (No. 40702020, 40972087), the Sichuan Youth Science & Technology Foundation (No. 09ZQ026-006) and the National Oil and Gas Special Project (No.XQ-2009-01).

REFERENCES

1. *Dyni, J. R*. Oil shale developments in the United States // Oil Shale. 2006. Vol. 23, No. 2. P. 97–98.
2. *Kök, M. V*. Oil shale resources in Turkey // Oil Shale. 2006. Vol. 23, No. 3. P. 209–210.
3. *Sukardjo, Hadiyanto*. Indonesian oil shale prospects and resources as an alternative energy // 26th Oil Shale Symposium, Golden, Colorado, 16 and 17 October 2006.

4. *Qian*, *J. L*. China's oil business is going ahead // Oil Shale. 2006. Vol. 23, No. 4. P. 295.
5. *Liu*, *Z. J*., *Yang*, *H. L*., *Dong*, *Q. S*., *Zhu*, *J. W*., *Guo*, *W*., *Ye*, *S. Q*., *Liu*, *R*., *Meng*, *Q. T*., *Zhang*, *H. L*., *Gan*, *S. C*. Oil Shale in China. – Beijing: Petroleum Industry Press, 2004. P. 98–167 [In Chinese with English abstract].
6. *Qian*, *J*., *Wang*, *S. L*. Oil shale development in China // Oil Shale. 2003. Vol. 20, No. 3S. P. 356–359.
7. *Wang*, *P. J*., *Wang*, *D. P*., *Chang*, *P*., *Li*, *H*. Metallic biomineralization of continental black shales // Journal of Changchun University of Earth Sciences. 1996. Vol. 26, No. 1. P. 47–53 [in Chinese with English abstract].
8. *Fu, X. G., Wang, J., Qu, W. J., Duan, T. Z., Du, A. D., Wang, Z. J., Liu, H*. Re-Os (ICP-MS) dating of marine oil shale in the Qiangtang basin, northern Tibet, China // Oil Shale. 2008. Vol. 25, No. 1. P. 47–55.
9. *Fu*, *X. G., Wang, J., Zeng, Y. H., Li, Z. X., Wang, Z. J.* Geochemical and palynological investigation of the Shengli River marine oil shale (China): Implications for paleoenvironment and paleoclimate // Int. J. Coal Geol. 2009. Vol. 78, No. 3. P. 217–224.
10. *Fu*, *X. G., Wang, J., Tan*, *F. W*., *Zeng*, *Y. H*. Sedimentological investigations of the Shengli River-Changshe Mountain oil shale (China): relationships with oil shale formation // Oil Shale. 2009. Vol. 26, No. 3. P. 373–381.
11. *Wang*, *W. F*., *Qin*, *Y*., *Sang*, *S. X*., *Zhu*, *Y. M*., *Wang*, *C. Y*., *Weiss*, *D. J*. Geochemistry of rare earth elements in a marine influenced coal and its organic solvent extracts from the Antaibao mining district, Shanxi, China // Int. J. Coal Geol. 2008. Vol. 76, No. 4. P. 309–317.
12. *Rantitsch*, *G*., *Melcher*, *F*., *Meisel*, *Th*., *Rainer*, *Th*. Rare earth, major and trace elements in Jurassic manganese shales of the Northern Calcaeous Alps: hydrothermal versus hydrogenous origin of stratiform manganese deposits // Miner. Petrol. 2003. Vol. 77, No. 1–2. P. 109–127.
13. *Dai*, *S. F*., *Li*, *D*., *Chou*, *C. L*., *Zhao*, *L*., *Zhang*, *Y*., *Ren*, *D. Y*., *Ma*, *Y. W*., *Sun*, *Y. Y*. Mineralogy and geochemistry of boehmite-rich coals: New insights from the Haerwusu Surface Mine, Jungar Coalfield, Inner Mongolia, China // Int. J. Coal Geol. 2008. Vol. 74, No. 3-4. P. 185–202.
14. *Qi*, *H. W*., *Hu*, *R. Z*., *Zhang*, *Q*. Concentration and distribution of trace elements in lignite from the Shengli Coalfield, Inner Mongolia, China: Implications on origin of the associated Wulantuga Germanium Deposit // Int. J. Coal Geol. 2007. Vol. 71, No. 2–3. P. 129–152.
15. *Condie*, *K. C*. Another look at rare earth elements in shales // Geochim. Cosmochim. Ac. 1991. Vol. 55, No. 9. P. 2527–2531.
16. *Ketris*, *M. P*., *Yudovich*, *Y. E*. Estimations of clarkes for carbonaceous biolithes: World averages for trace element contents in black shales and coals // Int. J. Coal Geol. 2009. Vol. 78, No. 2. P. 135–148.
17. *Wang, J., Tan, F. W., Li, Y. L., Li, Y. T., Chen, M., Wang, C. S., Guo, Z. J., Wang, X. L., Du, B. W., Zhu, Z. F*. The Potential of the Oil and Gas Resources in Major Sedimentary Basins on the Qinghai-Xizang Plateau. – Beijing: Geological Publishing House, 2004. P. 34–88 [in Chinese with English abstract].
18. *Yi*, *H. S*., *Deng*. *B*., *Xiong*, *S. P*. Lower Jurassic oil shale deposition from northern Tibet: chemostratigraphic signals and the early Toarcian anoxic event // 18th HKT Workshop Abstracts. 2003. P. 129–130.

19. *Kimura*, *T.* Relationships between inorganic elements and minerals in coals from the Ashibetsu district, Ishikari coal field, Japan // Fuel Process. Technol. 1998. Vol. 56, No. 1–2. P. 1–19.
20. General Administration of Quality Supervision, Inspection and Quarantine of the People's Republic of China. 2008. Proximate analysis of coal, GB/T212-2008. – Beijing: Standard Press of China, 2008. P. 4 [in Chinese].
21. General Administration of Quality Supervision, Inspection and Quarantine of the People's Republic of China. Determination of total sulfur in coal, GB/T214-2007. – Beijing: Standard Press of China, 2007. P. 4–8 [in Chinese].
22. General Administration of Quality Supervision, Inspection and Quarantine of the People's Republic of China. Determination of forms of sufer in coal, GB/T215-2003. – Beijing: Standard Press of China, 2003. P. 1–5 [in Chinese].
23. General Administration of Quality Supervision, Inspection and Quarantine of the People's Republic of China. Determination of total organic carbon in sedimentary rock, GB/T19145-2003. – Beijing: Standard Press of China, 2003. P. 2–4 [in Chinese].
24. *Mukhopadhyay*, *P. K.*, *Goodarzi*, *F.*, *Crandlemire*, *A. L.*, *Gillis*, *K. S.*, *MacNeil*, *D. J.*, *Smith*, *W. D.* Comparison of coal composition and elemental distribution in selected seams of the Sydney and Stellarton Basins, Nova Scotia, Eastern Canada // Int. J. Coal Geol. 1998. Vol. 37, No. 1–2. P. 113–141.
25. *Finkelman*, *R. B.* Trace and minor elements in coal // Organic Geochemistry / Engel, M. H., Macko, S. A. (Eds.). New York, NY: Plenum Press, 1993. P. 593–607.
26. *Haskin*, *L. A.*, *Haskin*, *M. A.*, *Frey*, *F. A.*, *Wilderman*, *T. R.* Relative and absolute terrestrial abundances of the rare earths // Origin and distribution of the elements / Ahrens, L. H. (ed.). Oxford: Pergamon, 1968. P. 889–911.
27. *Gromet*, *L. P.*, *Haskin*, *L. A.*, *Korotev*, *R. L.*, *Dymek*, *R. F.* The “North American shale composite”: Its compilation, major and trace element characteristics // Geochim. Cosmochim Ac. 1984. Vol. 48, No. 12. P. 2469–2482.
28. *Taylor*, *S. R.*, *Mcleman*, *S. M.* The Continental Crust: Its Composition and Evolution. – Oxford: Blackwell, 1985. P. 57–72.
29. *Eskenazy*, *G. M.* Rare earth elements in a sampled coal from the Pirin deposit, Bulgaria // Int. J. Coal Geol. 1987. Vol. 7, No. 3. P. 301–314.
30. *Schatzel*, *S. J.*, *Stewart*, *B. W.* Rare earth element sources and modification in the Lower Kittanning coal bed, Pennsylvania: implications for the origin of coal mineral matter and rare earth element exposure in underground mines // Int. J. Coal Geol. 2003. Vol. 54, No. 3–4. P. 223–251.
31. *Chatziapostolou*, *A.*, *Kalaitzidis*, S., *Papazisimou*, *S.*, *Christanis*, *K.*, *Vagias*, *D.* Mode of occurrence of trace elements in the Pellana lignite (SE Peloponnese, Greece) // Int. J. Coal Geol. 2006. Vol. 65, No. 1–2. P. 3–16.
32. *Webb*, *G. E.*, *Kamber*, *B. S.* Rare earth elements in Holocene reefal microbialites: a new shallow seawater proxy // Geochim. Cosmochim. Ac. 2000. Vol. 64, No. 9. P. 1557–1565.
33. *Brumsack*, *H.-J.* The trace metal content of recent organic carbon-rich sediments: Implications for Cretaceous black shale formation // Palaeogeogr. Palaeocl. 2006. Vol. 232, No. 2–4. P. 344–361.

Presented by A. Raukas
Received November 19, 2009